Title
Numerical Results on the Stability of a Drop Trapped between Parallel Planes

Author
Vogel, T.I.

Publication Date
1991-03-01

LBL-30486
Preprint

Lawrence Berkeley Laboratory
UNIVERSITY OF CALIFORNIA

Physics Division

Mathematics Department

To be submitted for publication

Numerical Results on the Stability of a Drop Trapped between Parallel Planes

T.I. Vogel

March 1991

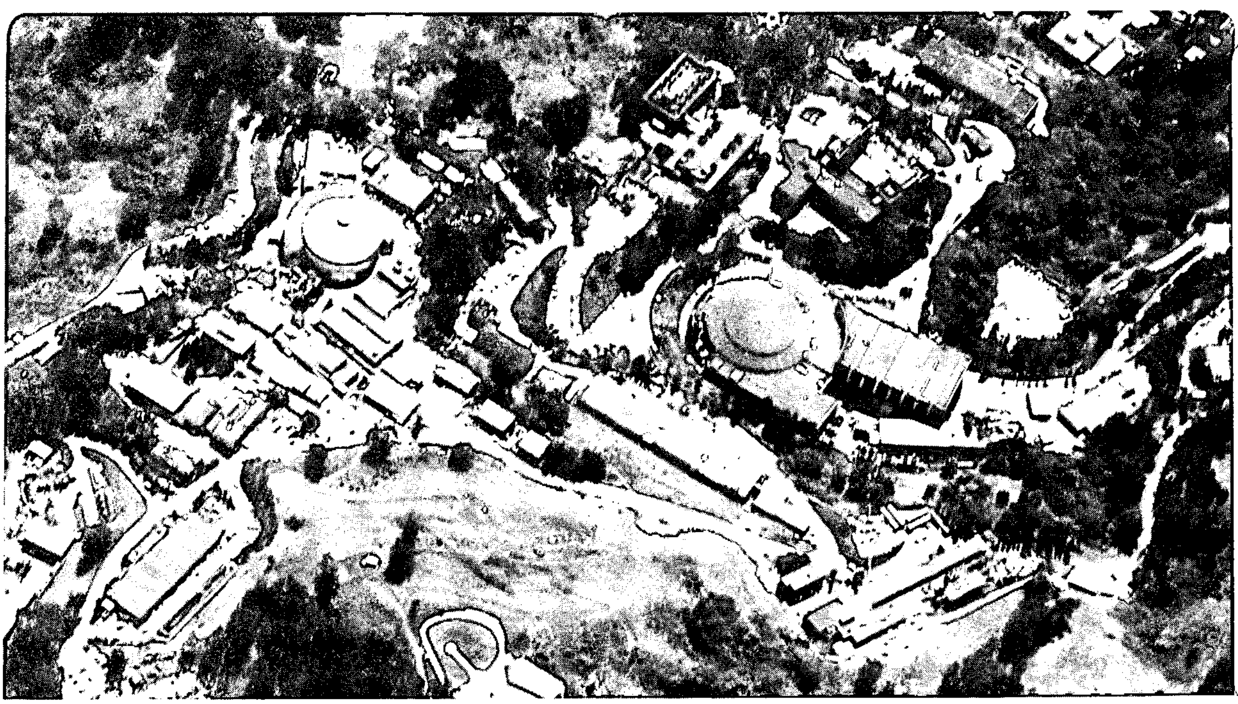

Prepared for the U.S. Department of Energy under Contract Number DE-AC03-76SF00098

DISCLAIMER

LBL-30486

NUMERICAL RESULTS ON THE STABILITY OF A DROP TRAPPED BETWEEN PARALLEL PLANES*

Thomas I. Vogel

Department of Mathematics
Texas A&M University
College Station, TX 77843
and
Lawrence Berkeley Laboratory
University of California
Berkeley, CA 94720

March 1991

* This work was supported in part by the National Science Foundation under grant DMS-8801515 and by the Applied Mathematical Sciences subprogram of the Office of Energy Research, U.S. Department of Energy, under contract DE-AC03-76SF-00098.

Numerical Results on the Stability of a Drop Trapped Between Parallel Planes

Thomas I. Vogel

§1. Introduction.

The physical situation considered in this paper is that of a drop of liquid forming a bridge between two parallel, homogeneous planes as in the picture below.

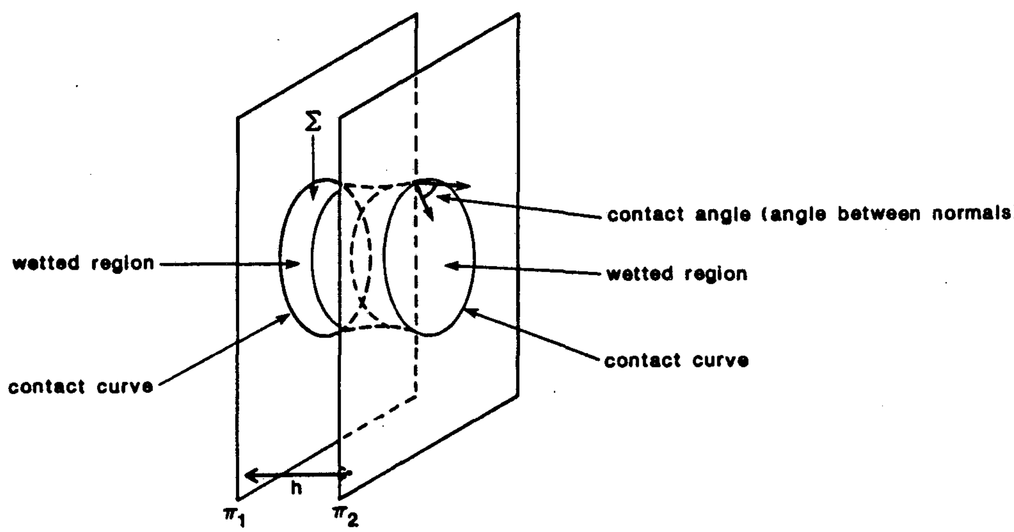

I am continuing work begun in [4] and [5], and the present paper is an expansion of the numerical results in §5 of [5].

We seek local minima of

$$I(f) \equiv 2\pi \int_0^h f\sqrt{1+(f')^2}dx - a_1\pi f^2(0) - a_2\pi f^2(h)$$

subject to the constraint

$$J(f) \equiv \pi \int_0^h f^2 dx = V \quad ,$$

where a_1 and a_2 are material constants, and V is the volume of the drop. From the first variation it follows that

$$\begin{aligned} \mathcal{M}(f) &\equiv \frac{1}{2}\left(\frac{f''}{(1+(f')^2)^{\frac{3}{2}}} - \frac{1}{f(1+(f')^2)^{\frac{1}{2}}}\right) = H, \\ f'(0) &= -\cot\gamma_1, \\ f'(h) &= \cot\gamma_2, \end{aligned} \tag{1.1}$$

for some constant H, where γ_1 and γ_2 are the (physically determined) contact angles with Π_1 and Π_2. Functions satisfying (1.1) are stationary but not necessarily stable. In [4] it is shown that if a solution to (1.1) satisfies the following two conditions, the drop it represents is stable.

1) The Sturm-Liouville problem

$$L(\psi) \equiv -\left(\frac{f\psi'}{(1+(f')^2)^{\frac{3}{2}}}\right)' - \frac{\psi}{f(+(f')^2)^{\frac{1}{2}}} = \lambda\psi,$$
$$\psi'(0) = \psi'(h) = 0$$

has precisely one negative eigenvalue, and

2) Suppose that $f(x) \equiv f(x;\epsilon_0)$ may be embedded in a smoothly parametrized family $f(x;\epsilon)$ of solutions to (1.1) with γ_1 and γ_2 fixed, but H depending on ϵ. Then the second condition for stability is that $H'(\epsilon_0)V'(\epsilon_0) > 0$, where $V(\epsilon)$ is the volume of the drop corresponding to $f(x;\epsilon)$.

If (1.2) has two negative eigenvalues, or if $H'(\epsilon_0)V'(\epsilon_0) < 0$, then the drop is not stable. The present paper investigates stability of trapped drops with varying contact angles using the above criteria.

§2. Explanation of H vs. V Plots (Figures 1 - 7)

The method of calculation is outlined in §5 of [5]. Some of the angles plotted also appeared in [5]. However, those graphs were prepared by a draftsman from computer plots. The graphs presented here are straight from a computer, and thus would not have been inadvertantly smoothed. The plots in the present paper were drawn by PICSURE using data generated as in [5].

Each point (H,V) on one of the curves represents the mean curvature and volume of a solution to (1.1). Figures 1 and 2 show that for $\gamma_1 = \gamma_2 = 20°$ and $\gamma_1 = \gamma_2 = 30°$, instability occurs before the appearance of an inflection on the boundary (which corresponds to the bifurcation. See §3.) For nearby unequal angles, the instability occurs at larger volumes, again due to condition 2 failing. One sees that the bifurcation of $\gamma_1 = \gamma_2$ splits as the contact angles become unequal. Although it is not apparent from these plots, the curves representing stable drops will have a vertical asymptote at H_∞, which will be one half of the curvature of the circular arc making the correct contact angles with $x = 0$ and $x = 1$. One can determine that $H_\infty = \frac{1}{2}(\cos\ \gamma_1 + \cos\gamma_2)$.

Figures 3 and 4 show that for $\gamma_1 = \gamma_2 = 40°$ and $\gamma_1 = \gamma_2 = 70°$, instability seems to occur because of condition 1 failing, i.e., we can reach the bifurcation (at which λ_1 changes sign) apparently before $\frac{dV}{dH}$ changes sign. The caveat is added since conceivably $\frac{dV}{dH}$ could change sign twice in the family of curves without inflections. Certainly this behavior was not observed, and for convex drops §4 of [5] proves that it cannot occur.

Figure 5 covers a larger area in the $H-V$ plane than the previous figures. It is easy to show that the $H-V$ curve for cylinders is $V = \frac{-\pi}{4H^2}$. I computed H vs. V for a number of unduloids with one inflection (the right-most curve marked *unduloid*). The rest of the unduloid curves may be obtained from the one-inflection family as follows. For the case

$\gamma_1 = \gamma_2 = 90°$, an unduloid with k inflections may obtained by lining up k copies of an unduloid with one inflection and then scaling. The picture below illustrates the process by taking 3 copies of an unduloid with one inflection (one reversed) to obtain an unduloid with three inflections on the interval [0,1].

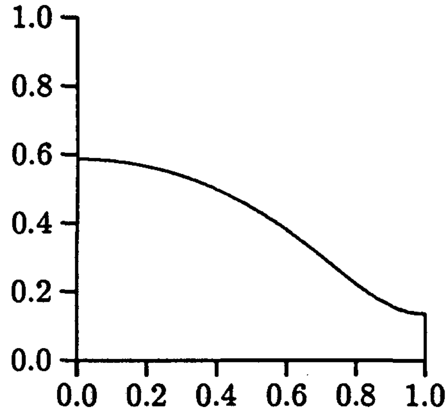

One inflection

$\Longrightarrow$

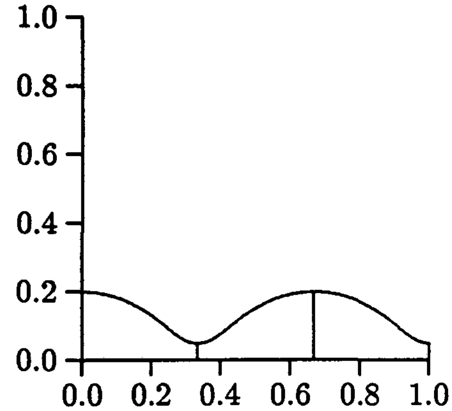

Three inflections

If (H, V) is the mean curvature of the " building block" unduloid, then the mean curvature and volume of the resulting unduloid is $(kH, \frac{1}{k^2}V)$. This scaling was used to construct the $H - V$ curves for the other families of unduloids.

Figures 6 and 7 show that drops for $\gamma_1 = \gamma_2 = 120°$ and $\gamma_1 = \gamma_2 = 140°$ are stable until the bifurcation. This is guaranteed by Theorem 4.2 of [5]. For $\gamma_1 = 119°, \gamma_2 = 121°$, instability is due to condition 2 failing. The previously mentioned theorem shows that an inflection must have appeared before this instability, and indeed this was observed numerically. In general, if $\gamma_1 = \gamma_2$, the appearance of an inflection signals the occurence of a bifurcation (see below), whereas if $\gamma_1 \neq \gamma_2$, these are unrelated.

§3. Investigation of Bifurcation for Equal Contact Angles

To investigate the bifurcation for equal contact angles, I exploited the fact that it coincides with the appearance of inflections on the boundary. This deserves a proof.

Theorem: *If $\gamma_1 = \gamma_2 \neq 90°$, then the profile with second derivative vanishing on the boundary represents a bifurcation between a family a zero-inflection profiles, a family of two-inflection profiles, and two families of one-inflection profiles.*

Proof: Using formulas from [2], the inclination angle ϕ_{inf} at the inflection for any unduloid will satisfy

$$\sin^2 \phi_{\text{inf}} = \left(\frac{r_{\max} - r_{\min}}{r_{\max} + r_{\min}}\right)^2,$$

where $r_{\max}$ is the maximum radius of the unduloid and $r_{\min}$ is the minimum radius of the unduloid. For the critical unduloid that I claim is the point of bifurcation, we must have

$$\sin^2\left(\frac{\pi}{2} - \gamma\right) = \left(\frac{r_{\max} - r_{\min}}{r_{\max} + r_{\min}}\right)^2,$$

where $\gamma_1 = \gamma_2 = \gamma$ is the contact angle. Recall that unduloids are obtained by tracing a focus of an ellipse as it is rolled without slipping along the axis of rotation. Therefore, $r_{\max}$ is $a+c$, and $r_{\min} = a-c$, where a, b, and c are the standard quantities for the ellipse generating the critical unduloid. Thus

$$\sin^2\left(\frac{\pi}{2}-\gamma\right) = \frac{c^2}{a^2}.$$

Keeping a fixed, we may increase c by a small amount, which will cause $|\phi_{\inf}|$ to increase from $|\frac{\pi}{2}-\gamma|$. This will split the points at which ϕ equals $\pm\left(\frac{\pi}{2}-\gamma\right)$ into two pairs, as in the picture below. The marked points are where the profiles have inclination $\pm 30°$, so that the unduloid would have contact angle $60°$ if cut there.

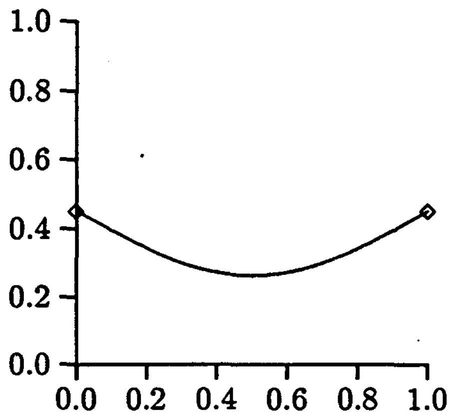

Critical unduloid for $\gamma = 60°$, with h=1

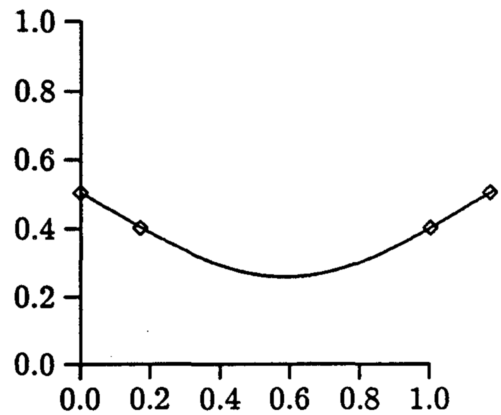

Increased c, same a

Taking one point from each pair and considering the part of the unduloid between these two points, we can obtain a section of the new unduloid with 0 or 2 inflections or two unduloids with one inflection. In general, the length of the section of the unduloid thus obtained will be close to but not equal to h. We must therefore scale the unduloid slightly to obtain a section of length h making the correct contact angles. By changing c an arbitrarily small amount, we obtain by this construction solutions to (1.1) with 0, 1, or 2 inflections uniformly close to the critical unduloid, showing that a bifurcation occurs.

Thus, to find V and H for the bifurcation point for $\gamma_1 = \gamma_2 = \gamma$ is the same as to find V and H for the unduloid for which an inflection point appears on the boundary. In general, computing the profile directly becomes quite difficult as we approach the bifurcation. I was able to avoid this difficulty by working with contact angles $\gamma_1 = \gamma$, $\gamma_2 = 90°$. By reflecting across the plane $x = h$, this corresponds to an unduloid making contact angles $\gamma_1 = \gamma_2 = \gamma$ on the planes $x = 0$ and $x = 2h$. Scaling, we see that a stationary surface with contact angles $\gamma_1 = \gamma, \gamma_2 = 90°$, mean curvature H and volume V corresponds to a stationary surface with $\gamma_1 = \gamma_2 = \gamma$, mean curvature $2H$ and volume $V/4$. The point of dealing with $\gamma_1 = \gamma$, $\gamma_2 = 90°$ is that for this case the appearance of an inflection on the left plane does not signal a bifurcation. We may, therefore, compute the profile with

$\gamma_1 = \gamma$, $\gamma_2 = 90°$ and an inflection at $x = 0$ without trouble, and then scale to find V and H for the bifurcation of $\gamma_1 = \gamma_2 = \gamma$.

Figure 8 shows the volume at the bifurcation for $\gamma_1 = \gamma_2 = \gamma$. The computed minimum occurs at 90°, agreeing with computations of W. C. Carter [1]. A proof of this fact will appear in [3]. Figure 9 shows the mean curvature at the bifurcation. Figure 10 combines the information in Figure 8 and 9. It is a parametrized curve in the $H - V$ plane, where $(H(\gamma), V(\gamma))$ is the location of the bifurcation point of $\gamma_1 = \gamma_2 = \gamma$.

Figure 11 and 12 concern the slope of the curve $\{0 \text{ inflections}\} \cup \{2 \text{ inflections}\}$ at the bifurcation. This is of interest, since if $\frac{dV}{dH}$ at the bifurcation is negative, instability must be due to condition 2 failing. I have computed that for $\gamma_1 = \gamma_2 < 31.14°$, $\frac{dV}{dH} < 0$ at the bifurcation, and for $\gamma_1 = \gamma_2 > 31.14°$, $\frac{dV}{dH} > 0$ at the bifurcation. Figure 12 indicates that the slope at the bifurcation is not monotone as a function of γ. In fact, the data indicate that at $\gamma = 90°$ there is a local minimum. As yet, this is unproven.

Acknowledgements: The author was partially supported by the National Science Foundation (DMS-8801515). Some of the research was performed at Lawrence Berkeley Laboratory supported by the Applied Mathematical Sciences Subprogram of the Office of Energy Research, U.S. Department of Energy, under Contract Number DE-AC03-76SF00098.

References

1. Carter, W. C., The forces and behaviour of fluids constained by solids, Acta Metallurgica, vol. 36, #8, pp. 2283-2292, 1988.
2. Concus, P., and Finn, R., The shape of a pendent liquid drop, Phil. Trans. Roy. Soc. London, ser. A, vol. 292, no. 1391, pp. 307-340, 1979.
3. Finn, R., and Vogel, T. I., The volume infimum for liquid bridges, in preparation.
4. Vogel, T. I., Stability of a liquid drop trapped between two parallel planes, SIAM J. Appl. Math., vol. 47, #3, pp. 516-525, 1987.
5. Vogel, T. I., Stability of a liquid drop trapped between two parallel planes II: general contact angles, SIAM J. Appl. Math., vol. 49, #4, 1989.

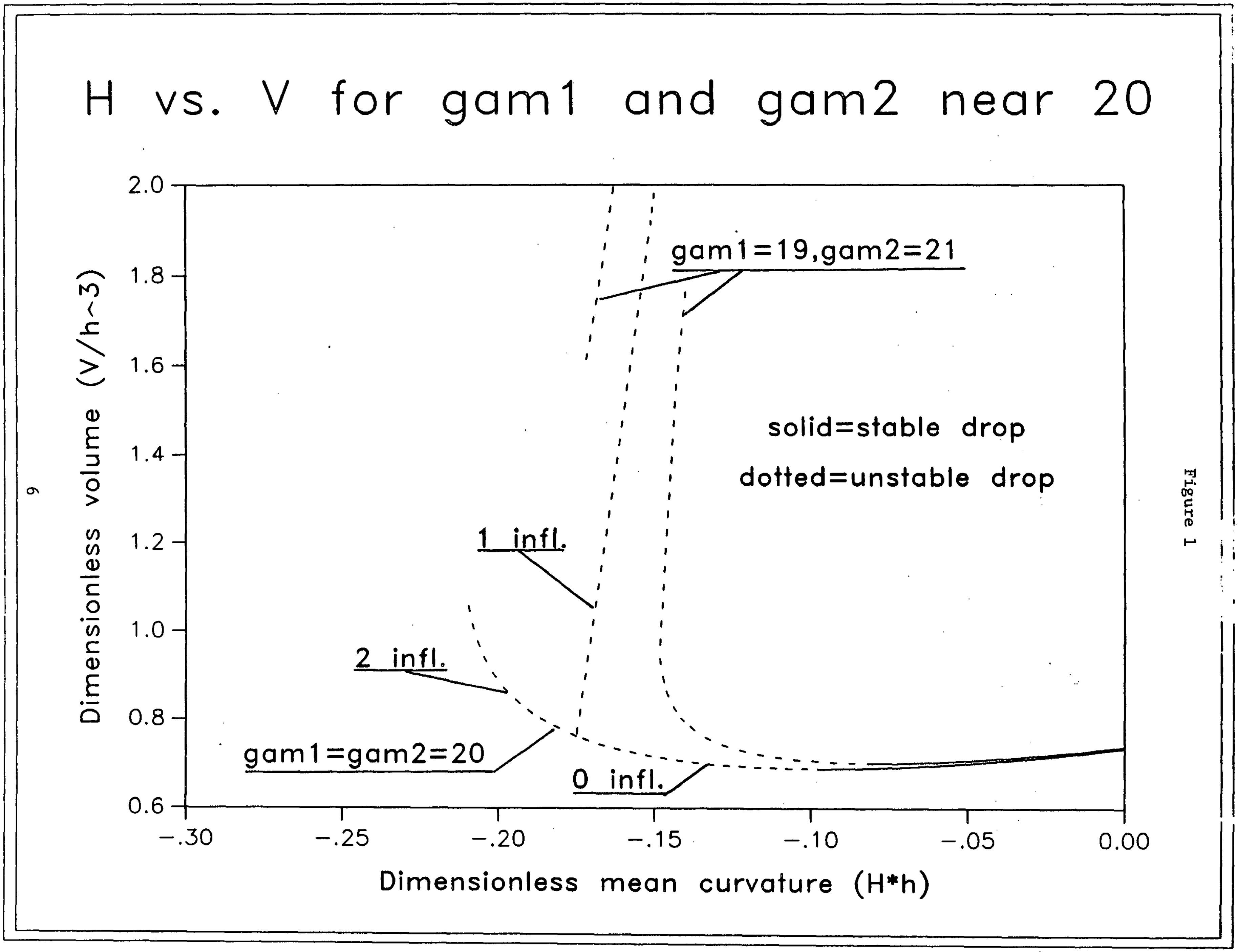

H vs. V for gam1 and gam2 near 20
Dimensionless volume (V/h^3)
2.0
1.8
1.6
1.4
1.2
1.0
0.8
0.6
-.30
-.25
-.20
-.15
-.10
-.05
0.00
Dimensionless mean curvature (H*h)
gam1=19,gam2=21
solid=stable drop
dotted=unstable drop
1 infl.
2 infl.
gam1=gam2=20
0 infl.

Figure 1

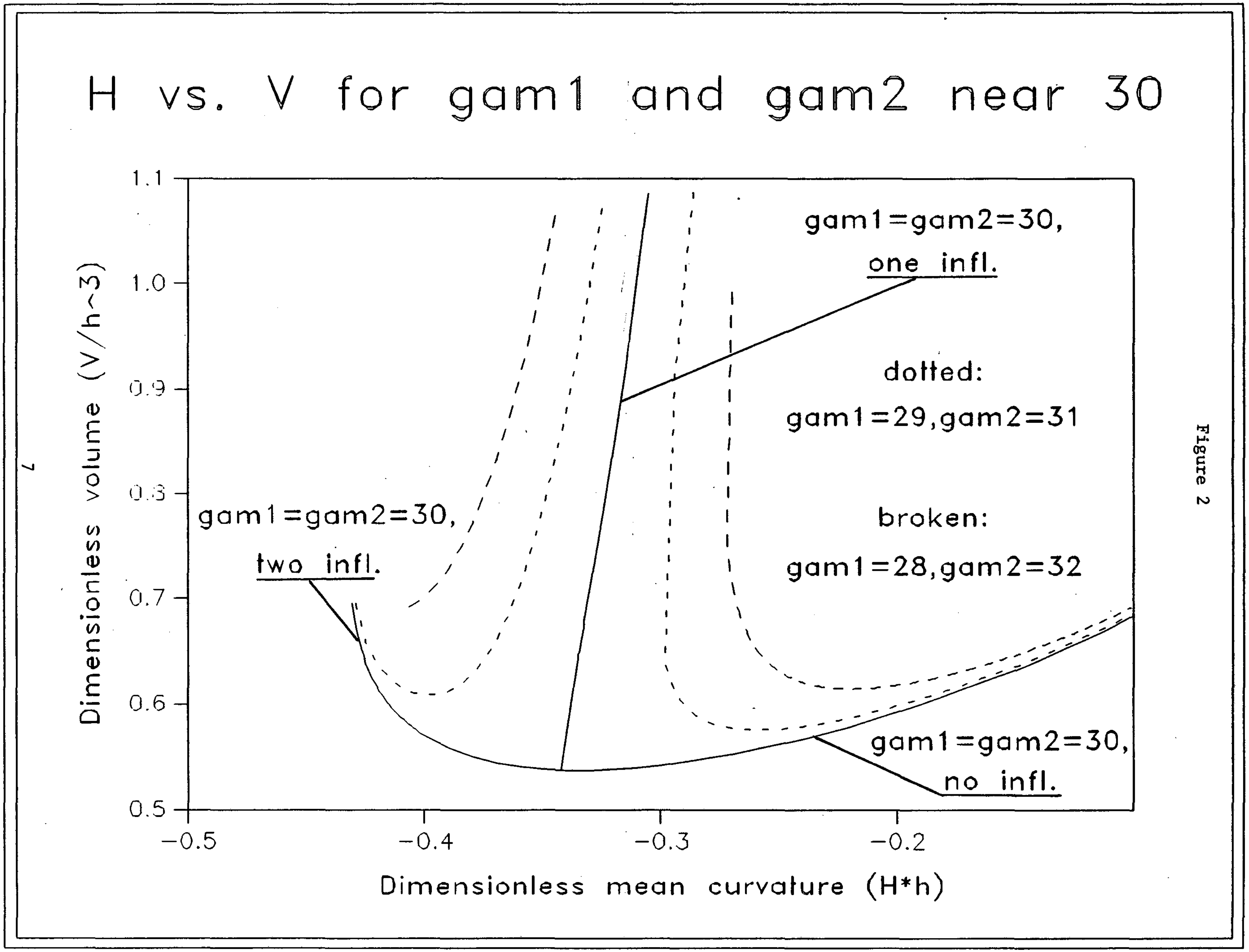

H vs. V for gam1 and gam2 near 30
1.1
1.0
0.9
0.8
0.7
0.6
0.5
−0.5
−0.4
−0.3
−0.2
Dimensionless volume (V/h^3)
Dimensionless mean curvature (H*h)
gam1=gam2=30,
one infl.
dotted:
gam1=29,gam2=31
broken:
gam1=28,gam2=32
gam1=gam2=30,
two infl.
gam1=gam2=30,
no infl.

Figure 2

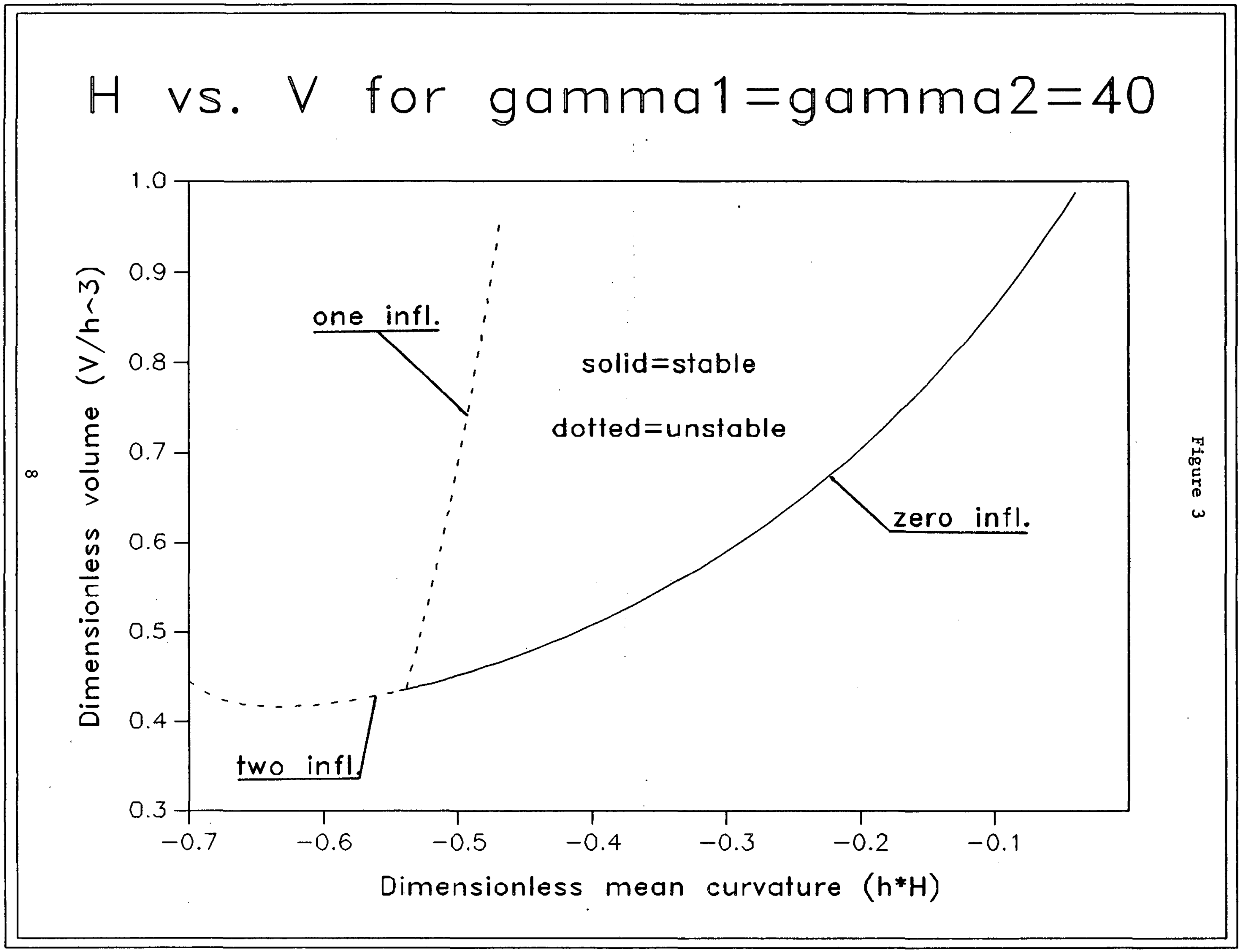
H vs. V for gamma1=gamma2=40
Dimensionless volume (V/h^3)
1.0
0.9
0.8
0.7
0.6
0.5
0.4
0.3
one infl.
solid=stable
dotted=unstable
zero infl.
two infl.
−0.7
−0.6
−0.5
−0.4
−0.3
−0.2
−0.1
Dimensionless mean curvature (h*H)

Figure 3

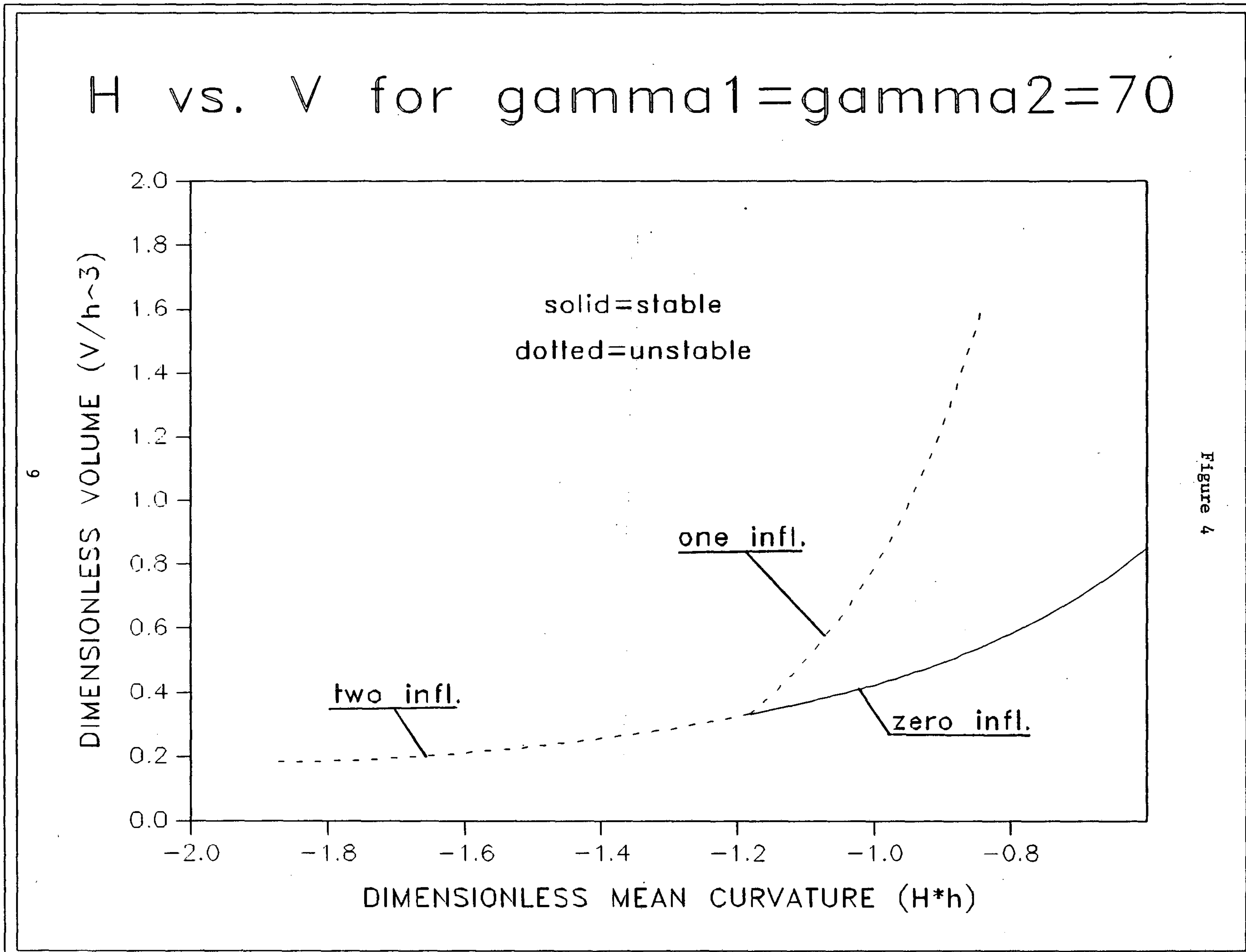
H vs. V for gamma1=gamma2=70
solid=stable
dotted=unstable
one infl.
two infl.
zero infl.
DIMENSIONLESS VOLUME (V/h~3)
DIMENSIONLESS MEAN CURVATURE (H*h)
0.0
0.2
0.4
0.6
0.8
1.0
1.2
1.4
1.6
1.8
2.0
−2.0
−1.8
−1.6
−1.4
−1.2
−1.0
−0.8

Figure 4

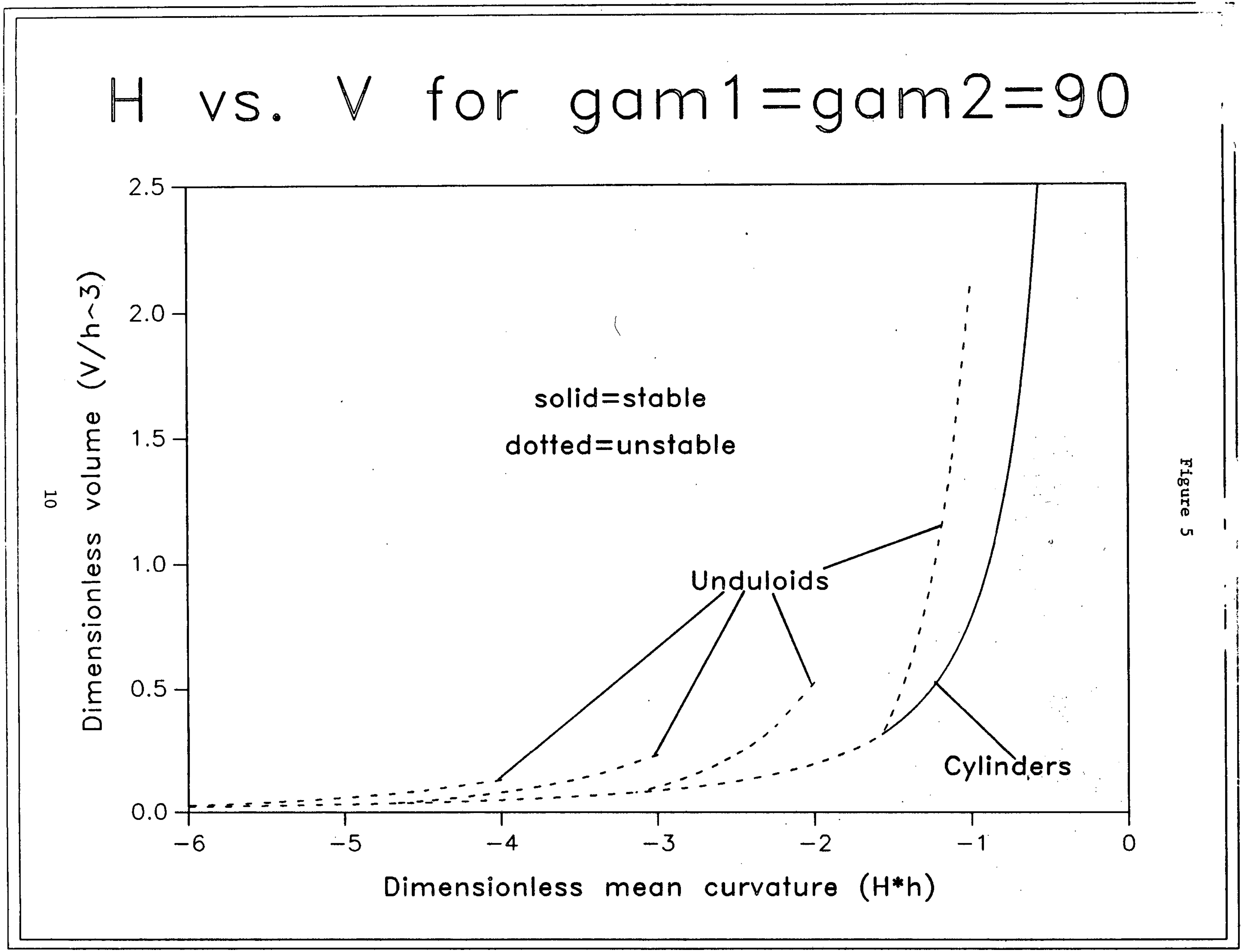

H vs. V for gam1=gam2=90
solid=stable
dotted=unstable
Unduloids
Cylinders
Dimensionless volume (V/h^3)
Dimensionless mean curvature (H*h)
2.5
2.0
1.5
1.0
0.5
0.0
−6
−5
−4
−3
−2
−1
0

Figure 5

Figure 6

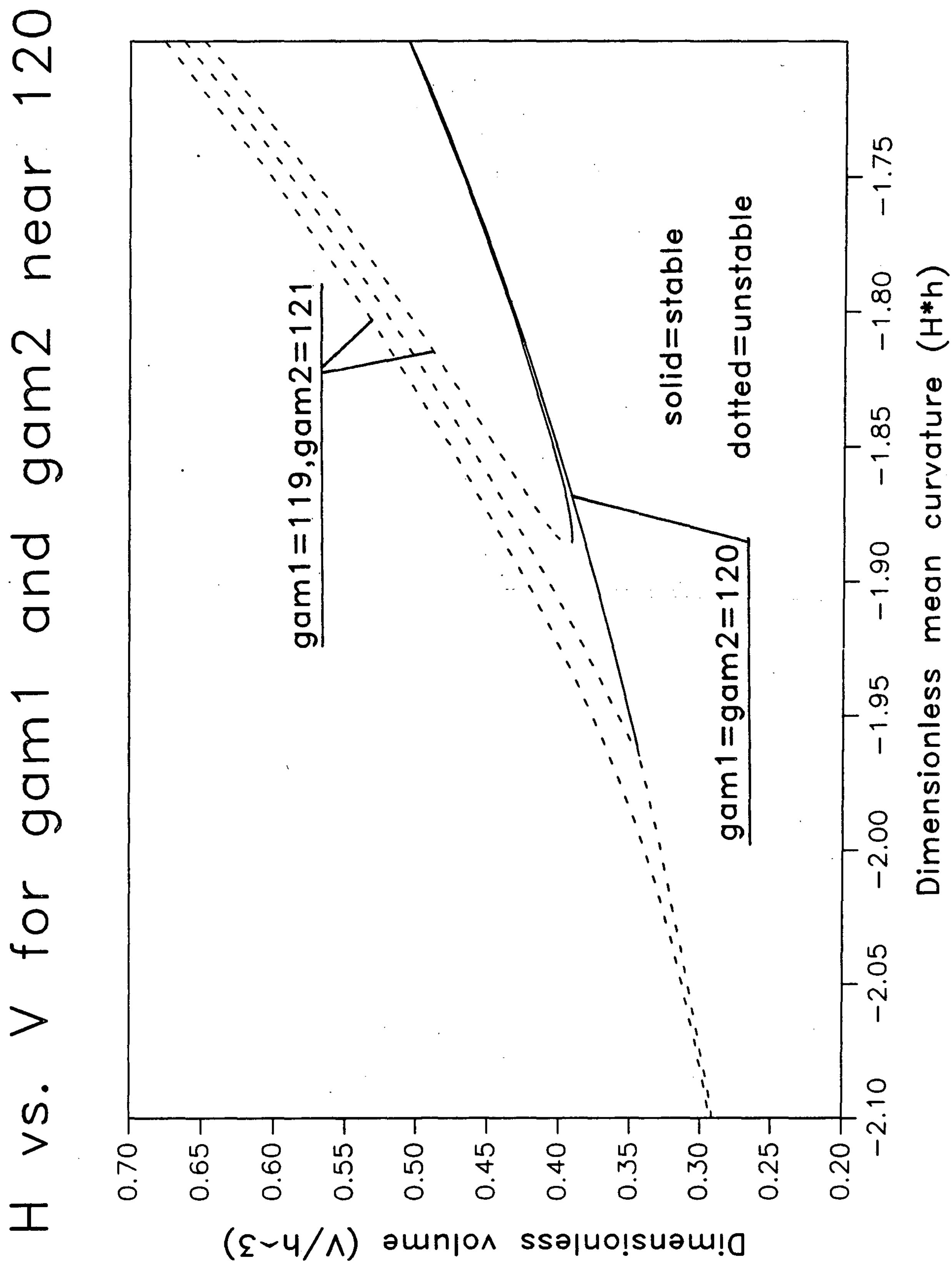
H vs. V for gam1 and gam2 near 120
gam1=119,gam2=121
gam1=gam2=120
solid=stable
dotted=unstable
Dimensionless mean curvature (H*h)
Dimensionless volume (V/h~3)
-2.10
-2.05
-2.00
-1.95
-1.90
-1.85
-1.80
-1.75
0.20
0.25
0.30
0.35
0.40
0.45
0.50
0.55
0.60
0.65
0.70

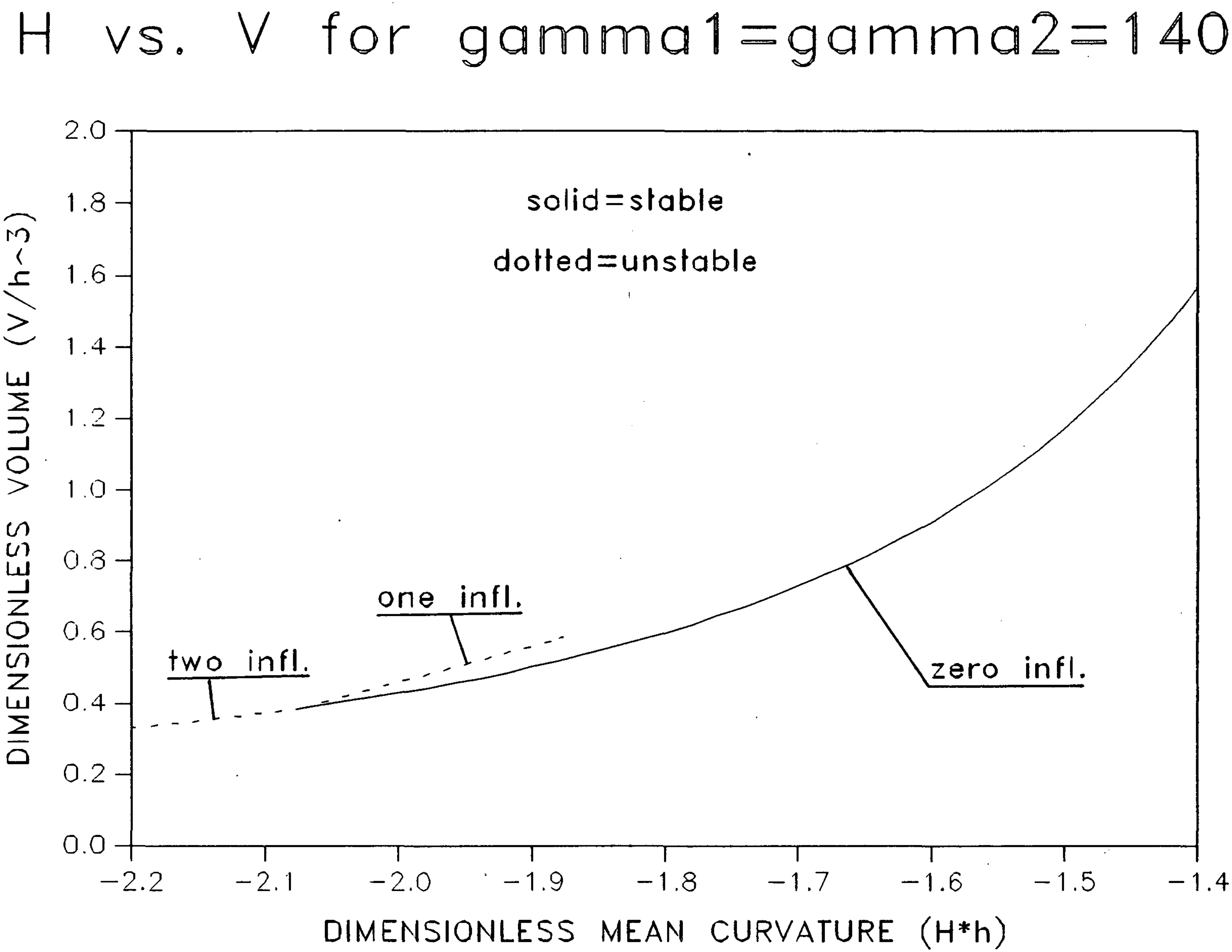
H vs. V for gamma1=gamma2=140
solid=stable
dotted=unstable
one infl.
two infl.
zero infl.
DIMENSIONLESS VOLUME (V/h~3)
DIMENSIONLESS MEAN CURVATURE (H*h)
2.0
1.8
1.6
1.4
1.2
1.0
0.8
0.6
0.4
0.2
0.0
-2.2
-2.1
-2.0
-1.9
-1.8
-1.7
-1.6
-1.5
-1.4

Figure 7

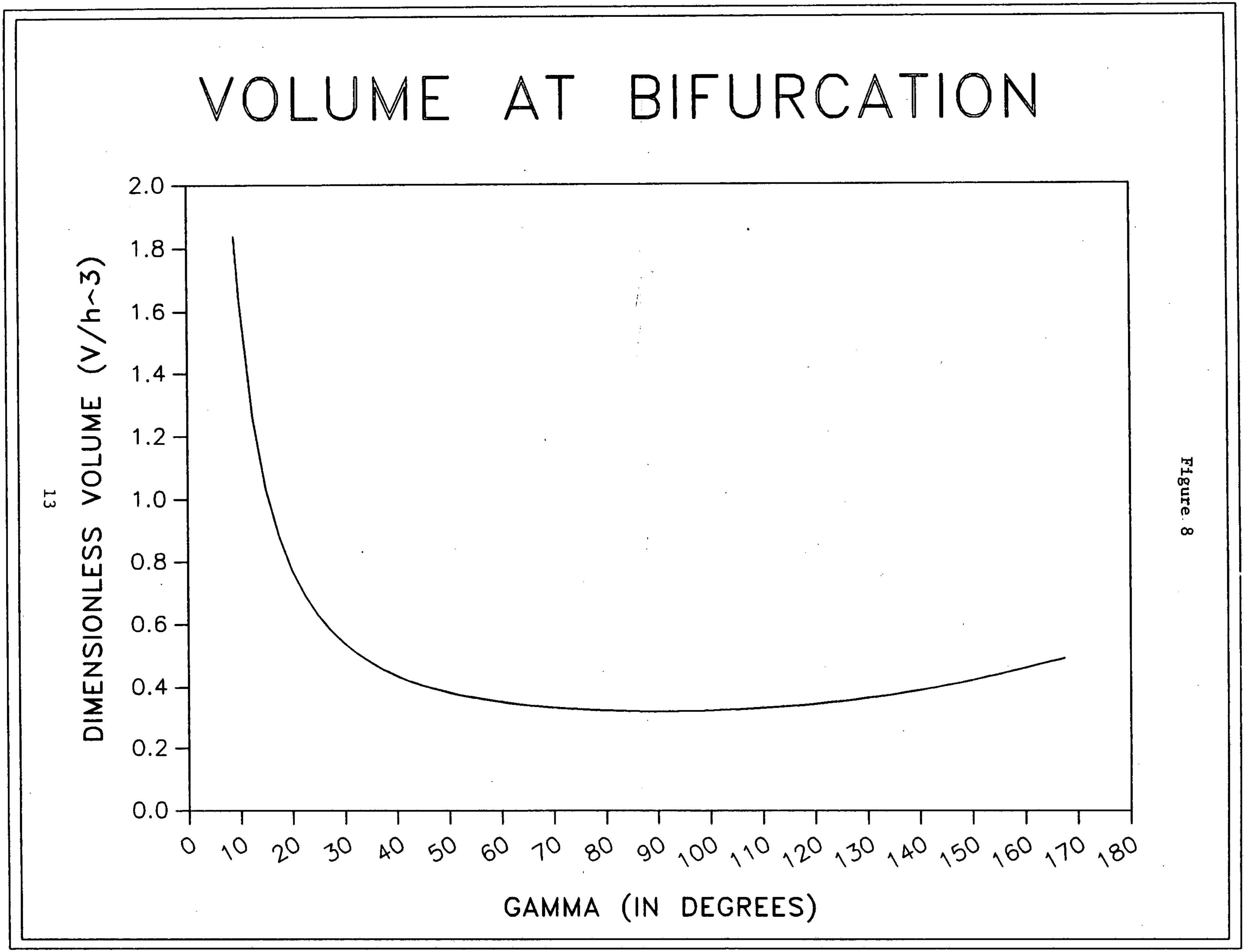
VOLUME AT BIFURCATION
DIMENSIONLESS VOLUME (V/h~3)
2.0
1.8
1.6
1.4
1.2
1.0
0.8
0.6
0.4
0.2
0.0
0
10
20
30
40
50
60
70
80
90
100
110
120
130
140
150
160
170
180
GAMMA (IN DEGREES)

Figure 8

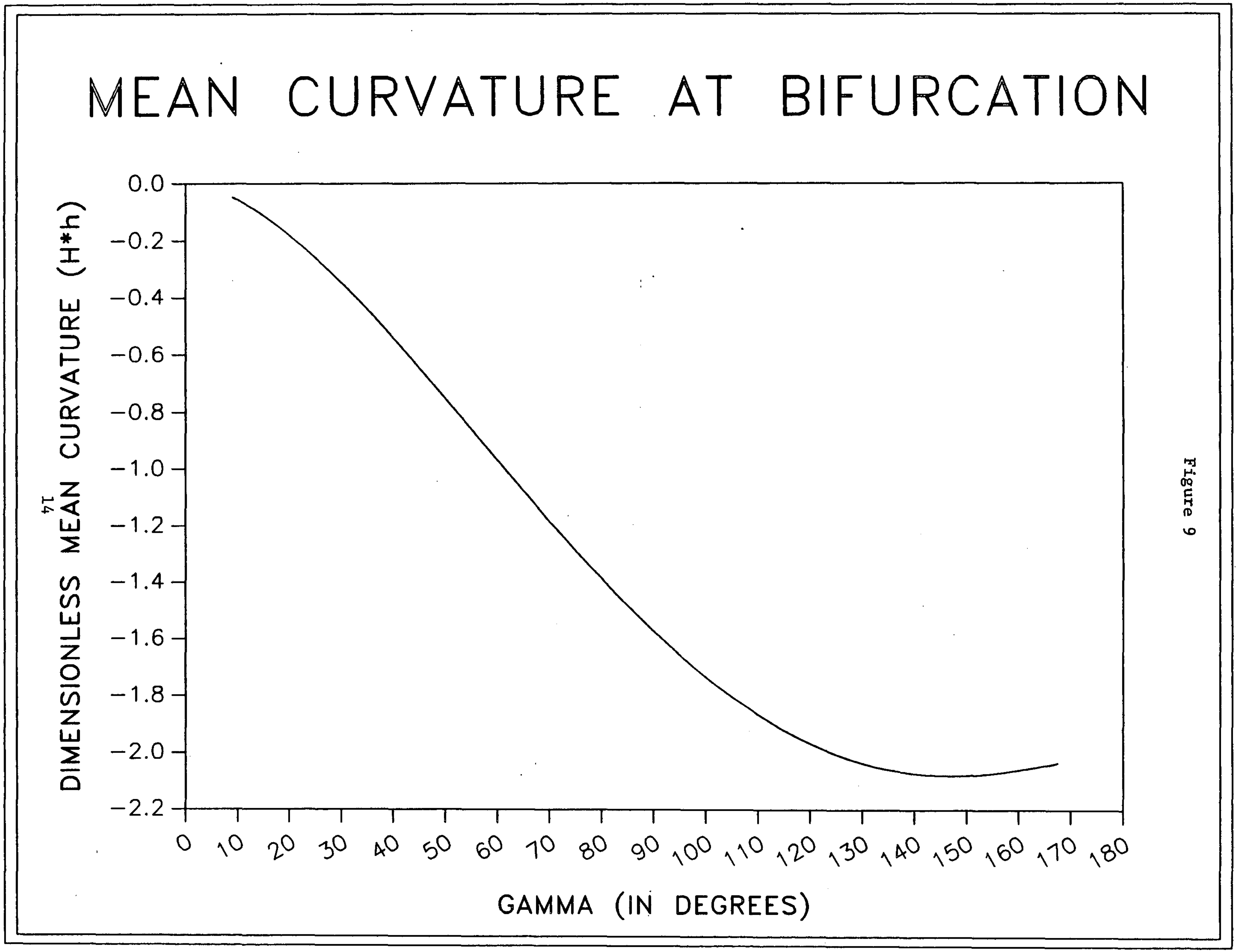
MEAN CURVATURE AT BIFURCATION
DIMENSIONLESS MEAN CURVATURE (H*h)
0.0
−0.2
−0.4
−0.6
−0.8
−1.0
−1.2
−1.4
−1.6
−1.8
−2.0
−2.2
0
10
20
30
40
50
60
70
80
90
100
110
120
130
140
150
160
170
180
GAMMA (IN DEGREES)

Figure 9

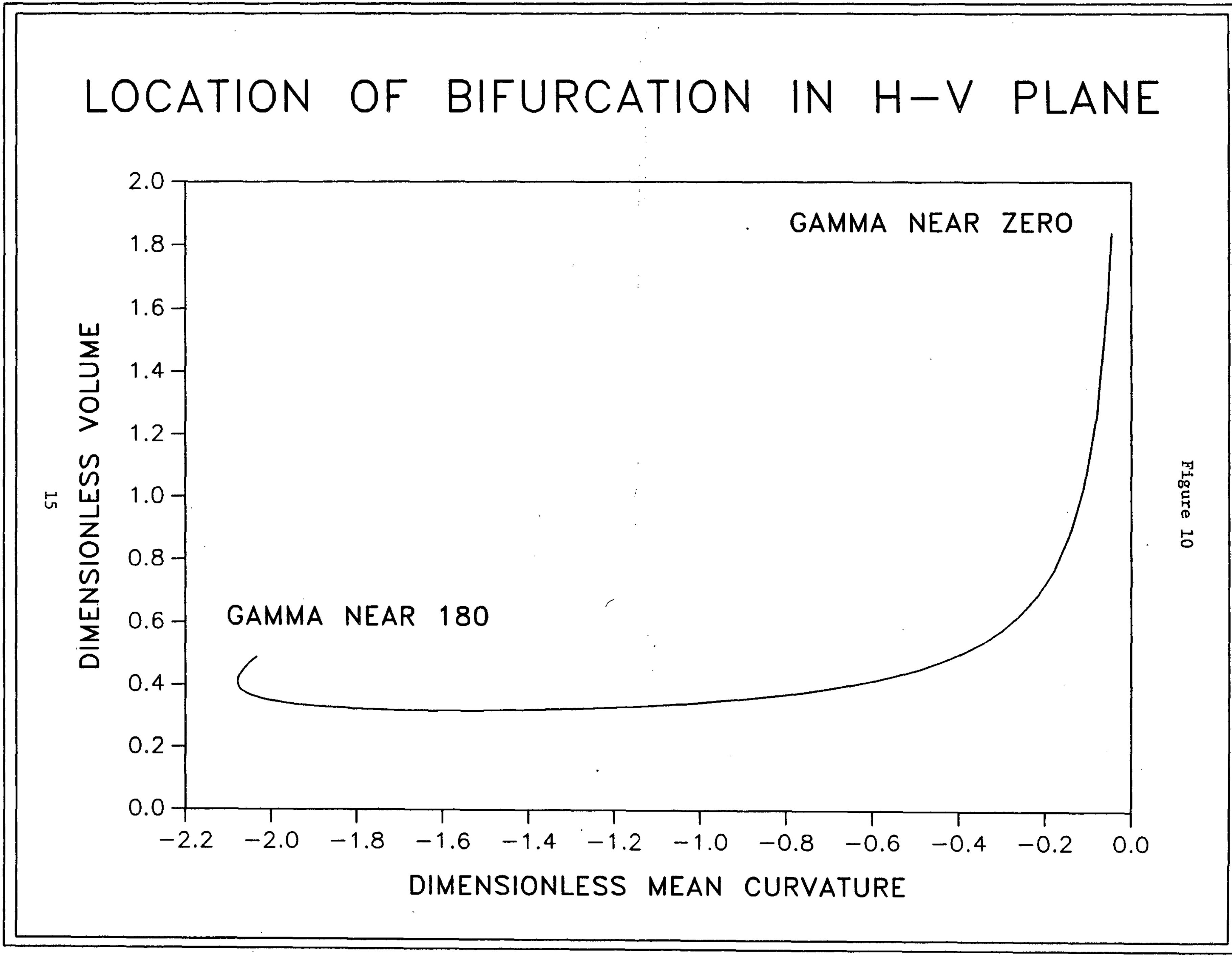
LOCATION OF BIFURCATION IN H-V PLANE
GAMMA NEAR ZERO
GAMMA NEAR 180
DIMENSIONLESS VOLUME
DIMENSIONLESS MEAN CURVATURE
2.0
1.8
1.6
1.4
1.2
1.0
0.8
0.6
0.4
0.2
0.0
−2.2
−2.0
−1.8
−1.6
−1.4
−1.2
−1.0
−0.8
−0.6
−0.4
−0.2
0.0

Figure 10

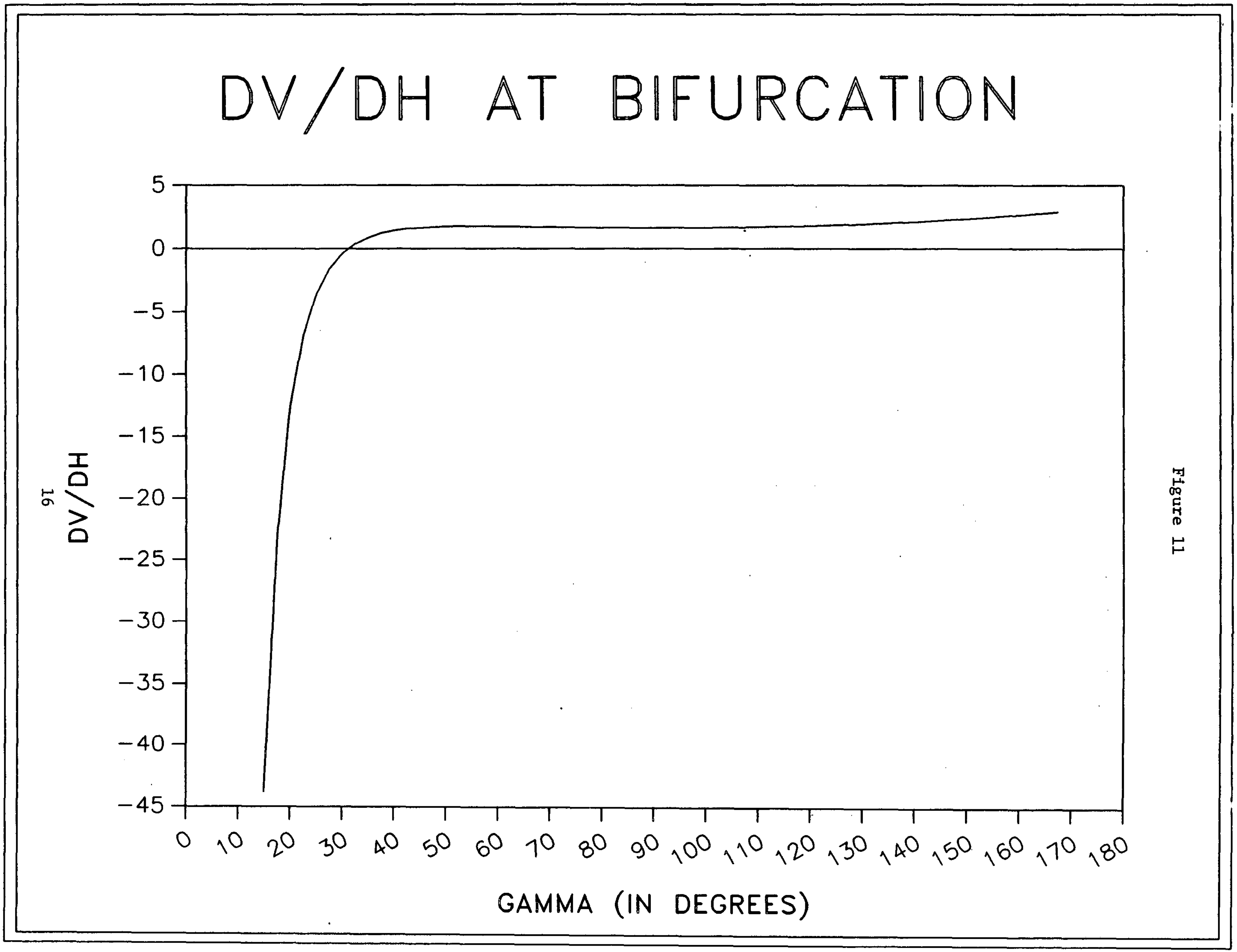

DV/DH AT BIFURCATION
5
0
−5
−10
−15
−20
−25
−30
−35
−40
−45
16
DV/DH
0
10
20
30
40
50
60
70
80
90
100
110
120
130
140
150
160
170
180
GAMMA (IN DEGREES)

Figure 11

Figure 12

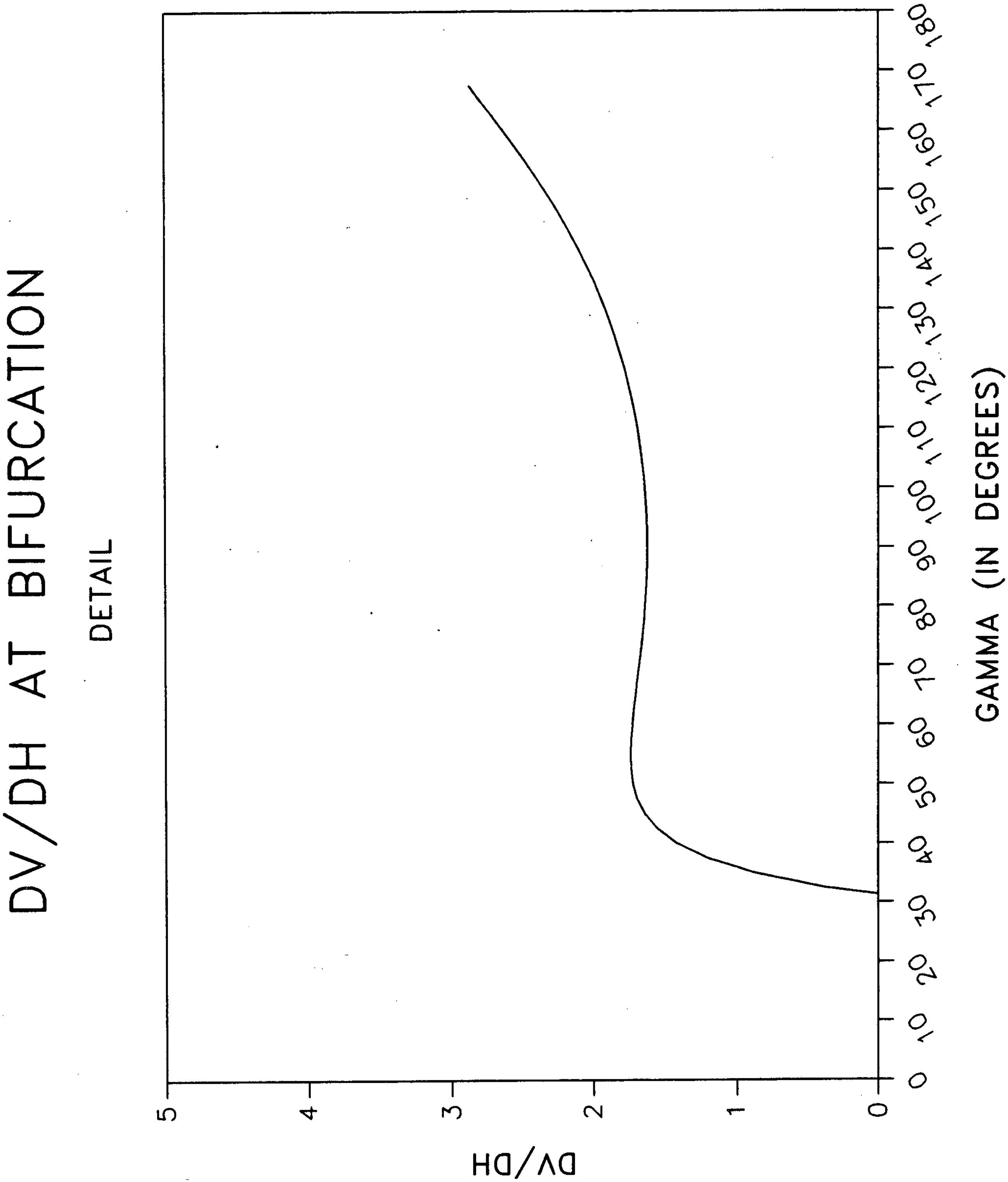
DV/DH AT BIFURCATION
DETAIL
DV/DH
0
1
2
3
4
5
GAMMA (IN DEGREES)
0
10
20
30
40
50
60
70
80
90
100
110
120
130
140
150
160
170
180